Electronic Supplementary Material (ESI) for Physical Chemistry Chemical Physics.
This journal is © the Owner Societies 2015

Electronic Supporting Information (ESI)

The use of The Rx spin label in Orientation Measurement on Proteins, by EPR.

M. A. Stevens[a], J. E. McKay[b], J. L. S. Robinson[a], H. EL Mkami[b], G. M. Smith[b] and D. G. Norman[a*]

[a.] *Nucleic Acid Structure Research Group, College of Life Sciences, University of Dundee, Dow Street, Dundee DD1 5EH, UK.*
[b.] *School of Physics and Astronomy, University of St Andrews, St. Andrews, KY16 9SS UK*

** corresponding Author*

Content

Table S5 Field positions of the pump and observe pulses for each w-band PELDOR experiment on site Rx19-20sample.
Table S6 Field positions of the pump and observe pulses for each w-band PELDOR experiment on site Rx26-27sample.
Figure S11 Experimental PELDOR signal, pulse excitation overlaid on the RX spin label spectrum (middle) and FFT of the PELDOR signal for each w-band orientation selective PELDOR experiment of sample RX19-20.
Figure S12 Experimental PELDOR signal, pulse excitation overlaid on the RX spin label spectrum (middle) and FFT of the PELDOR signal for each w-band orientation selective PELDOR experiment of sample RX26-27.

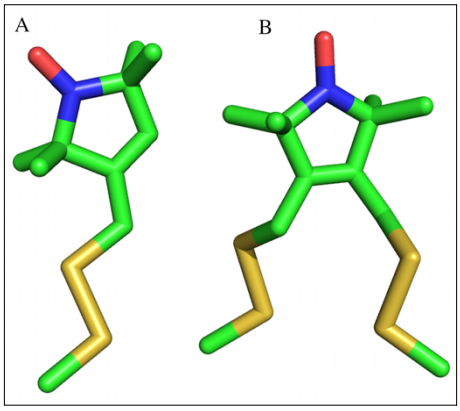

Fig S1. The structure of spin labels R1 and Rx and the label attachment sites on the protein Vps75. (A) Structure of R1, (B) structure of Rx

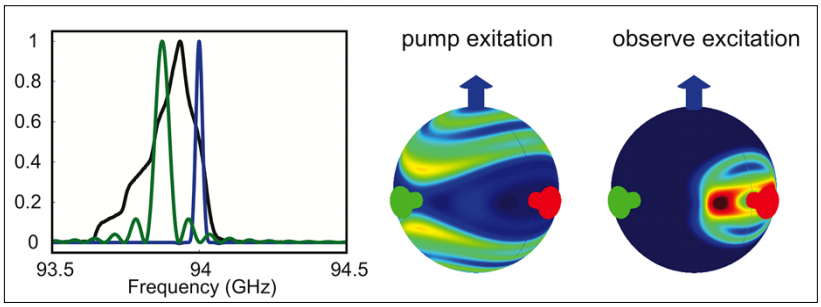

Fig S2. Diagram showing Left: typical W-Band RX spin label spectrum (black) with typical pump pulse excitation profile (green) and observe pulse profile (blue). Field offset = 0G, pump pulse offset = -45. Right: The corresponding orientation selection of the spin label relative to the magnetic field direction. Field used was 3.3435T

S1 Materials and Methods

Cloning, Expression and Purification of Vps75 Mutants:

Mutated plasmid vectors (a gift from Tom Owen-Hughes, Collage of life sciences, University of Dundee) were replicated in XL1-Blue cells (Agilent) and purified using the Qiagen miniprep kit and the relevant protocol. Success of the mutations were determined by DNA sequencing performed by the DNA sequencing and services (MRCPPU, College of life sciences, University of Dundee, Scotland,

www.dnaseq.co.uk) on a Biosystems model 3730 automated capillary DNA sequencer using Applied Biosystems Big-Dye Ver 3.1 chemistry.

The pET30a-Vps75 plasmid expression vectors were transformed into competent BL21 (DE3) Rosetta 2 cells (Novagen) Cells were cultivated at 37°C overnight in 20ml of luria broth (LB) media containing 50μg ml^{-1} of kanamycin and 50μg ml^{-1} chloramphenicol for selection. Cultivated cells were grown up at 37°C in 1L of LB media containing 50μg ml^{-1} of kanamycin and 50μg ml^{-1} chloramphenicol for selection. Upon reaching a OD_{600} of 0.8 cultures were induced by making them up to 1 mM isopropyl β-D-1-thiogalactopyranoside (IPTG) and cultures were left to express at 24 °C overnight

Cells were harvested by centrifuging at 4845 x g rcf for 20 minutes, the media was removed and the cell pellet was suspended in 5ml of binding buffer (500mM NaCl and 20mM Tris-HCl pH7.5) containing protease inhibitors E64, pepsin, AEBSF and aprotinin. Cells were burst by flash freezing in liquid nitrogen followed by sonication using 6 x 10 second pulses with 40 second rests on ice at full amplitude. Cell debris was removed from the samples by centrifuging at 35562 x g rcf for 30 minutes. Remaining debris were removed from the supernatant by filtration using a 0.45 μm filter (Sartorius Ministart GF hydrophilic) and loaded onto 2 ml of his-pur cobalt resin (Thermo Scientific). The beads were washed with 40ml of binding buffer followed by 40 ml of binding buffer containing 25 mM imidazole. Vps75 was eluted from the column using 8 ml of binding buffer containing 500 mM imidazole. Fractions were checked for Vps75 using 12% SDS-PAGE with the gel stained with a coomassie stain.

Purified protein samples were concentrated down using a 10 kDa cutoff concentration column (millipore) to a final volume of around 800 microl. Samples were made up to 50 mM dithiothreitol (DTT) and incubated at room temperature for 1 hour. DTT was removed by size exclusion chromatography on a sephadex S75 column equilibrated in binding buffer. Fractions containing Vps75 were pooled and the protein concentration was determined by measuring the samples absorption at 280 nm (thermo scientific nanodrop, 2000c) using a extinction coefficient of 49850 M^{-1} cm^{-1} predicted by Expasy [1]. Spin labeling was performed by the addition of 0.5 molar equivalents of 20mM 3,4-Bis-(methanethiosulfonylmethyl)-2,2,5,5-tetramethyl-2,5-dihydro-1H-pyrrol-1-yloxy (3,4 bis MTSSL) stock dissolved in dimethylformamide (DMF) to binding site every five minutes to a total amount of 2 equivalents. The labeling reaction was incubated at room temperature and left for a further hour after the final aliquot of spin label had been added.

Most of the excess spin label was removed by dialysis in a 10kDa cut-off membrane tubing against 1L of binding buffer overnight at 4 °C followed by two buffer changes at 3hr intervals. Samples for CW were further dialyzed using 10kDa cut-off membrane against 500ml of binding buffer at room temperature for 2 weeks with the buffer changed twice daily. To prevent microbial growth the dialysis buffer made up to 0.005% w/v sodium azide while the protein samples were made up to 0.05% w/v sodium azide.

EPR spectroscopy

CW: Samples contained 150 μM protein in binding buffer containing 30% w/w sucrose. Measurements were carried out on 10 μl of sample in 0.64mm ID, 0.8mm OD borosilicate capillary tubes, sealed with silicone gel. Spin label

efficiencies were determined by CW EPR using a dilution series of a known concentration of 4'-amino-TEMPO (4-Amino-2.2.6.6-tetramethylpiperidine-1-oxyl).

CW spectra were taken on a Bruker EMX spectrometer working at X-band using a super high sensitivity probe head (ER4122SHQE). CW was performed in a critically coupled resonator with a typical Q factor of 7000. Experiments were collected over 100 G centered at 3519 G in a constant microwave frequency of 9.876 GHz. Background noise was averaged out over 10 sweeps at a power of 10mW with a 2048 point resolution. The 2Azz' values were analyzed by measuring the spectral width between the center of the furthest left peak and the furthest right trough of the spectra.

Pulsed EPR: PELDOR samples were made up in binding buffer in a 1:1 ratio of D_2O to D_8 glycerol with a final concentration of spin label pairs of 100 to 150 μM the average sample size was 100 μl for both X and W bands. X-band samples were measured in 4.0mm OD, 3.0mm ID Quarts tubes (Norell S-4-EPR-250S).

PELDOR experiments were performed on a Bruker ELEXSYS E580 spectrometer, operating at X-Band, with a second Bruker 400U microwave source unit. Experiments were carried out in a MD4 dielectric ring resonator that was over-coupled to give a Q factor of approximately 100. Measurements were made at 50K where the sample is in a frozen glassy state with a video bandwidth set to 20MHz.

Samples were analyzed using the four pulse dead-time free PELDOR sequence with the pump π pulse frequency positioned at the center of the nitroxide spectrum and the frequency increased by 80 MHz for the observer pulse. The pulse sequence typically had a pump π-pulse between 12 and 18 ns with the observer π-pulse being 32 ns. The experiment repetition time was 4.08 ms with 50 shots at each time point and a number of scans sufficient to give a suitable signal to noise ratio.

W-band: Orientation PELDOR measurements were made at W-band (94GHz) using HIPER a home-built 1kW pulsed-EPR spectrometer, which has been described in a previous publication [2]. This system has subsequently been modified and now uses a non-resonant sample-holder operating in reflection, in induction mode, instead of a Fabry-Perot resonator. Samples are initially deposited into a 29mm deep, 3mm O.D., 2mm I.D fluorinated ethylene propylene (FEP) tube (Adtech Plolymer Engineering Limited). These are then placed inside a 3mm diameter circular waveguide transmission line, which is fed by a corrugated pipe transmission line. This allows for easier sample handling and increased sample volume and better concentration sensitivity than the Fabry-Perot system.

This non-resonant system has a 3dB operating bandwidth of ~800MHz., principally defined by the bandwidth of the source and thus has a relatively flat frequency response across the full nitroxide spectrum at W-band. Despite being non-resonant the system has an effective conversion factor of 0.6 G/W-1/2, similar to that achieved by Bruker MD4 x-band cavities. It also uses comparable sample volumes, to those used at X-band, resulting in a large increase in concentration sensitivity for PELDOR measurements.

The multi-wavelength sized sample can be sensitive to dielectric losses and dielectric scattering within the sample. Dielectric losses are expected to be negligible at the cryogenic temperatures used in the experiments, but dielectric scattering can occur if cracks or fractures are induced in the frozen glass during freezing. To minimize these effects the sample is annealed after sample loading.

The liquid Helium flow cryostat (Oxford Instruments) containing the transmission waveguide and sample holder was precooled to 150K prior to sample loading. The sample contained in a FEP tube was flash frozen in liquid nitrogen before being transferred into a pre-cooled sample holder.
To minimize the effect of cracks and fractures induced in the sample during freezing, the sample was annealed within the cryostat. Annealing was achieved by warming the cryostat to a temperature of ~180K which corresponds to the 'glassy state transition' of the 1:1 D_2O:D8 glycerol mix. Once the transition is achieved the sample was cooled to 60K. All experiments were performed at 60K.
Field swept echo spectrum measurements were performed using a spin echo sequence with optimized pulse lengths and pulse separation of 400ns. Pulse lengths were increased in later field sweep spectra measurements to reduce the effects of instantaneous diffusion.
PELDOR experiments were conducted using the dead-time free 4-pulse variant based around refocused echo. The primary coherent oscillator was kept at 94GHz and the secondary ELDOR oscillator was tuned to various offsets to achieve selection of different portions of the Rx spin label spectrum. The field was simultaneously tuned by the use of a ±1800G sweep coil. Pulse separations varied between experiments but were generally extended to the maximum time window yielding suitable signal to noise.

Orientation PELDOR Analysis: All the analysis is based around orientation selection PELDOR signal simulation code which has been home-written using the MATLAB package. The highly parallelized simulation code used 5000 spin pairs per simulation, generated to have relative rotation angles and positions according to the model parameters. For each of the spin pairs in the simulation the magnetic field vector direction was averaged over a set of 700 uniform distributed angles, taken from the 2-angle 'Repulsion set' [3]. Where there was a uniform library of relative rigid spin label pair conformations the uniform ZCW 3-angle set containing 6044 angles was used [4].
Parameters for the nitroxide g-tensor and hyperfine-tensor were derived by fitting to the field swept echo spectra and are shown in table S3.
The modulation depth analysis compared each simulation of the modulation depths in the uniform library set to the experimentally measured modulation depths. An RMSD value was calculated for each case and angle plots were produced based on these values. It was found that there was the expected experiment symmetries for each RMSD minimum, these relate to underlying experiment symmetries.
The fitting algorithm used genetic algorithm GA fitting functions included in the relevant MATLAB package toolbox. The fitting algorithm used the calculated RMSD between the experiment measured PELDOR signal and the current iteration PELDOR signal as a penalty for fitting. The fitting algorithm was allowed to vary all of the angles through their full range, and the distance

distribution was allowed to vary ±10A. Each of the angles and distance was given a distribution modeled as a normal distribution, which the fitting algorithm could vary up to a standard deviation of 90degrees. The distance and angles were not correlated in the simulated model, it was assumed that the spread in the orientation would result in a little variation between the distances for each conformer.
It was found that 1000 generation with 25 populations gave reliable and reproducible minimum. The algorithm was seeded with angles derived from the modulation depth analysis. It was checked that using random starting points it was possible to reach the same minimum however it took many more generations to reach.

Molecular Dynamics.: Rx was built onto a PDB structure of Vps75 PDB ID: 2ZD7 and molecular dynamics were carried out using Xplor-NIH. The backbone molecules for all residues except Rx were restrained using harmonic restraints with the only other restraint being Van der Waals Radius of the molecule. Dynamics were equilibrated by a 200 step minimization followed by a 2 ns dynamics varlet at 600 K, followed by a 2 ns dynamics varlet at 500 K. Dynamics were performed at 400 K with coordinate files pulled off at 2 ns time steps with dynamics ran for 4 micro s.
To describe the conformational distributions and assess the suitability of each site for the use of orientation dependent PELDOR, The orientations of each MD frame was express as a set of three rotations. These rotations orientated the label into a pre-determined conformation in relation to the protein backbone. Measurements were performed by first representing the spin label as two vectors. The first vector, named the nitrogen vector, ran from the mid point between the label binding sites C alphas to the nitrogen of the nitroxide. The second vector, named the C-C vector, was between the two carbons neighboring the nitroxide nitrogen. The direction of this vector was from the carbon closest to the lowest numbered attachment site residue to the carbon closest to the highest numbered attachment site residue. The first two transformations place the nitrogen vector perpendicular to either the helical axis of a α-helix or the plane of a β-sheet. The final transformation then rotates the C-C vector so it is parallel to the vector between the two binding site C alphas.
Angles used for this transformation were measured by first assigning a local coordinate frame to each secondary structural feature, with the origin at the mid point between the C alphas of the attachment site. In all cases the Y-axis is a vector between the two alpha carbons of the binding site running from the lowest to the highest residue number. The X-axis points in the direction that the nitrogen vector is aligned with after transformations have been performed. On α-helical binding sites the X-axis points away from the secondary structural feature so that it was orthogonal to both the Y-axis and a helical axis defined in the same manner as Kahn [5]. In β-sheet binding sites the X-axis is orthogonal to the Y-axis and perpendicular to the plane of the β-sheet at the coordinate set origin. The Z-axis runs in a direction to produce a right hand Cartesian coordinate system and is orthogonal to both the X and Y-axis.
The three angles for the transformation were labeled the Tilt, Twist and Roll with angle measurements performed on the pair of vectors representing the

label. These were carried out in the order Tilt, Twist then Roll, with the vectors rotated through each angle before making the next measurement. The Tilt was the rotation the nitroxide vector underwent around the Y-axis to bring it into the X-Y plane with the vector was pointing in a positive X direction. The Twist was the rotation of the nitrogen vector about the Z-axis to align it with the X-axis. The Roll was the rotation about the X-axis that placed the C-C vector in the same direction as the Y-axis and parallel to the X-Y plane. All rotations were measured in an anti clockwise direction.

Angles were measured for each site using the conformations of the spin label from the molecular dynamics run. A distribution was produced by pooling the measurements into 4 degree bins with the data point for each bin plotted at the start of its region. The data points were fitted by Gaussian distributions and angle distributions were represented as going from -180 degrease to 180 degrease (Figures 4 and S8).

These specific rotations were used to quantify the different ways the spin label can move. The tilt represents a back and forth motion around the axis of its binding site. The twist is a sideways motion along the labels binding site axis and the Roll is the rotation of the label around the nitroxide bond (see Figure S4). The distributions of the 3 angles seem to adequately illustrate the conformational flexibility of the spin labels at different attachment sites

Simulation of the MD derived distributions: Simulations of the orientations derived from MD, were performed by using a MATLAB script to calculate the relative orientation angles for the spin labels at each site to every partner at the other labeled site using their atom coordinate PDB files. Using these relative angles and their associated distance it was possible to directly input these into a version of the home-written PELDOR signal simulation code previously described.

Data Analysis: X-band PELDOR data was analyzed using DEERAnalysis2013 [6] using Tikhonov regularization. The regularization parameter was determined using an L curve with the parameter determined as that on the bend of the L. Where there was more than one bend in the curve a point towards the center of the first bend was chosen in order to prevent over smoothing of the distance distribution.

Distance distributions were obtained from the molecular dynamics by measuring the distance between the nitrogen on one side of each protein structure to all the positions of the nitrogen on the other side. These distributions were then binned at 0.5 Å intervals. Binned data was plotted against experimental distance distributions determined by PELDOR using a double Y-axis.

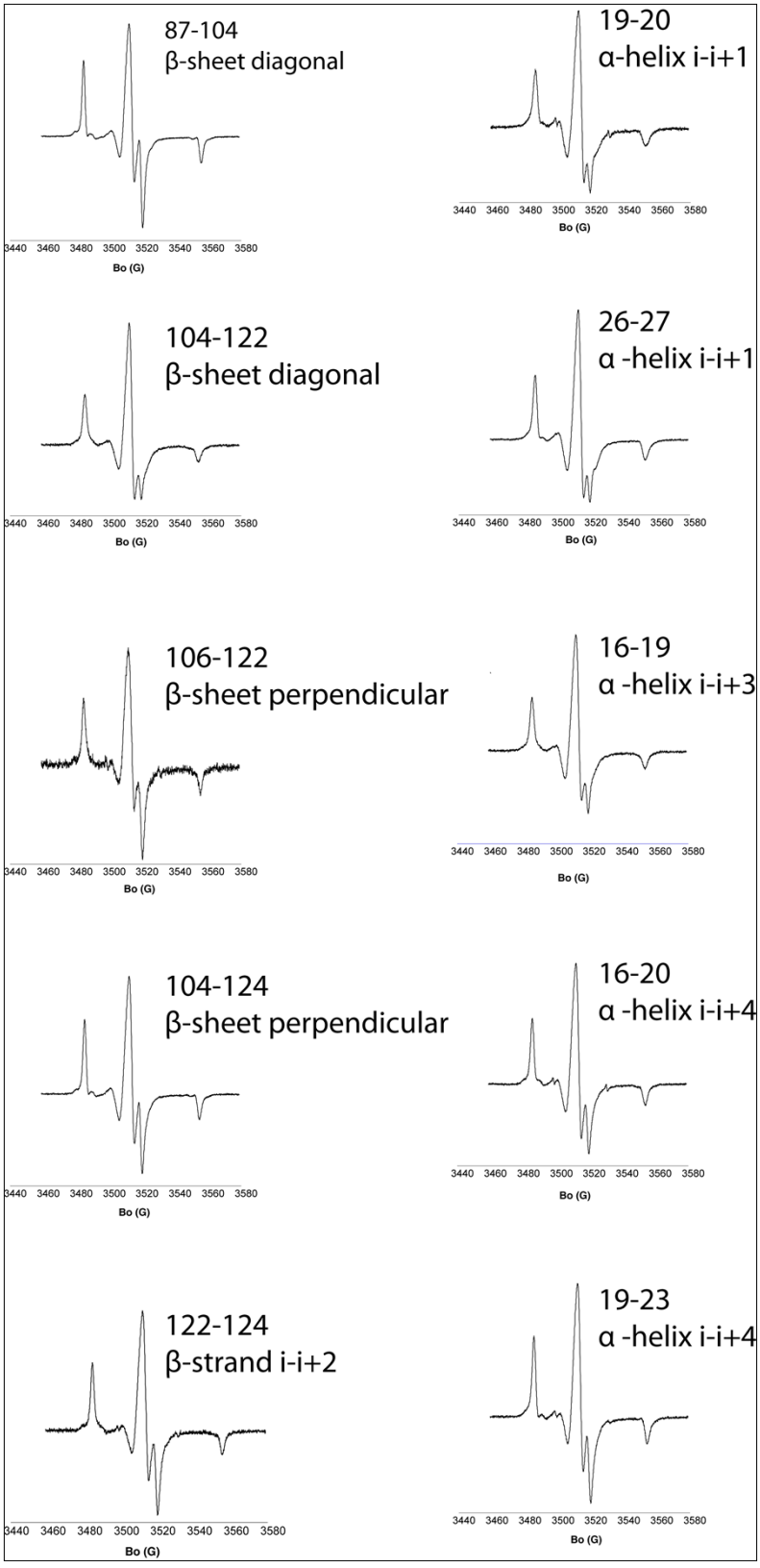

Fig. S3 Room temperature CW EPR spectra for all Rx label positions studied

Table S1. $2A_{zz}'$ values for the Rx labels at different attachment sites

Rx attachment sites	$2A_{zz}'$ (Gauss)	$2A_{zz}'$ (MHtz)
19-20 α-helix i-i+1	67.111	188
26-27 α -helix i-i+1	66.660	186
16-19 α -helix i-i+3	68.333	192
16-20 α -helix i-i+4	68.590	192
19-23 α -helix i-i+4	68.667	192
87-104 β-sheet diagonal	71.288	200
104-122 β-sheet diagonal	68.815	193
106-122 β-sheet perpendicular	70.803	198
104-124 β-sheet perpendicular	69.608	195
122-124 β-sheet i-i+2	70.890	199

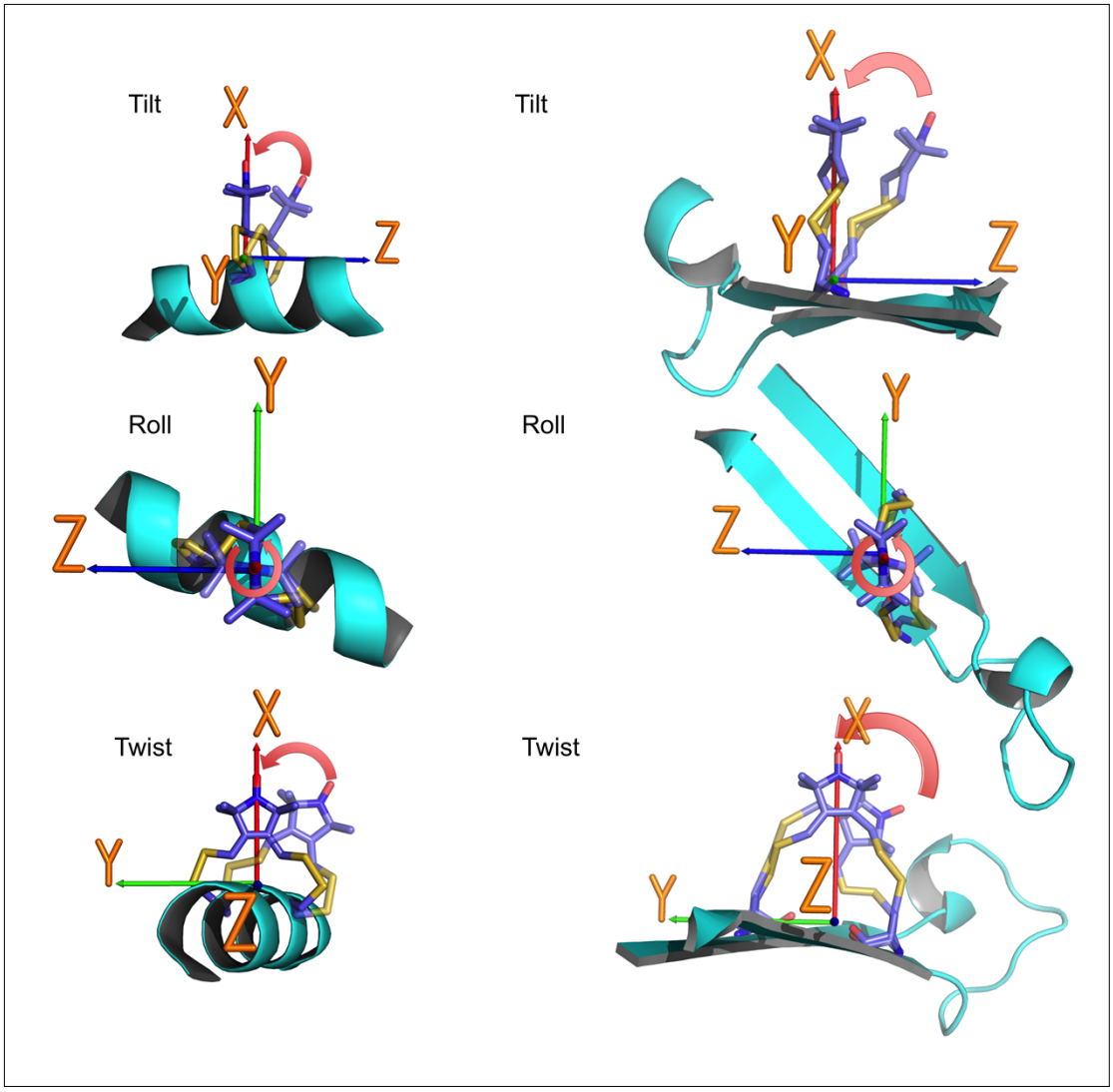

Fig. S4 A series of images representing the Tilt, Twist and Roll angles at the both the α-helix and β-sheet binding sites. The arrows on the diagram show the angle and the motion of the spin label associated with each rotation.

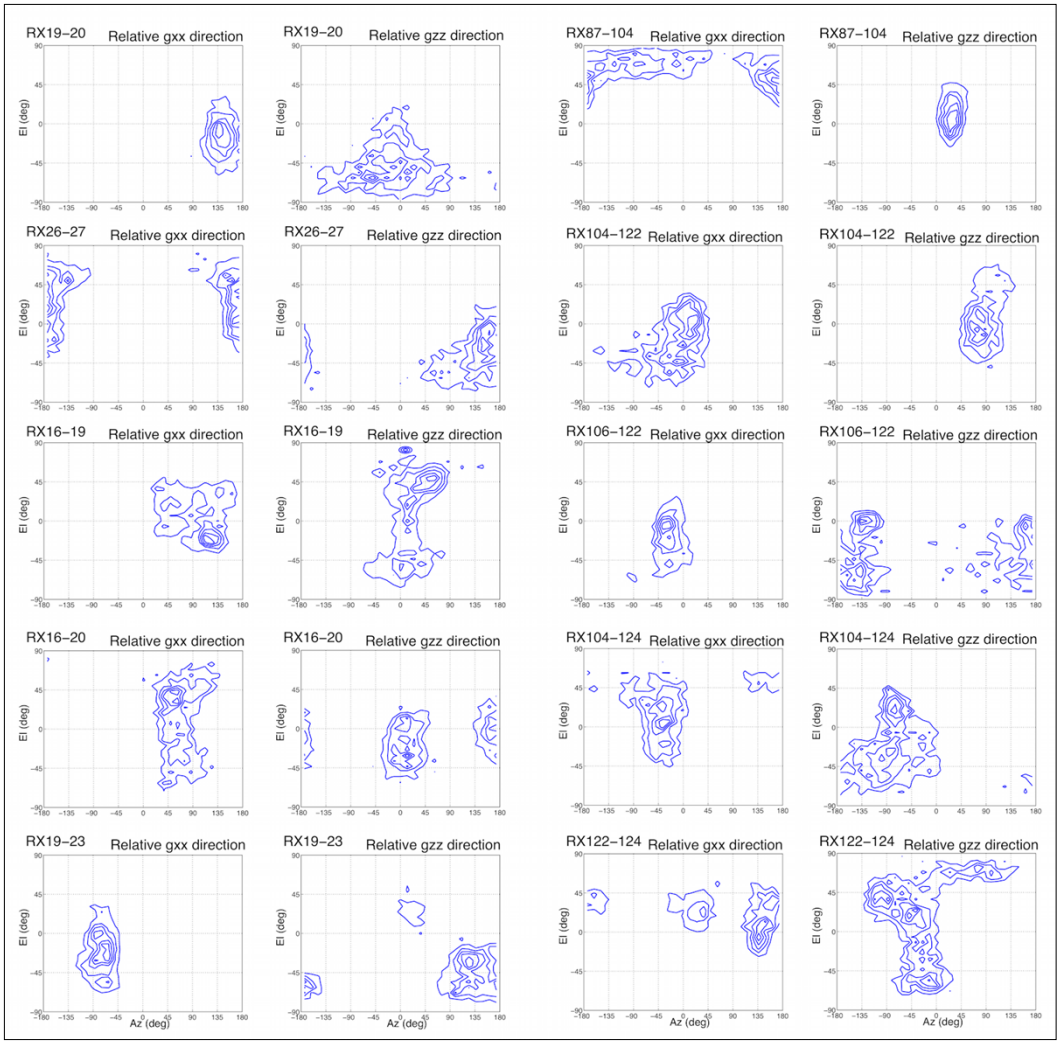

Fig. S5 Contour plots showing the relative rotation of the N-O vector, taken from MD frames for all Rx constructs.

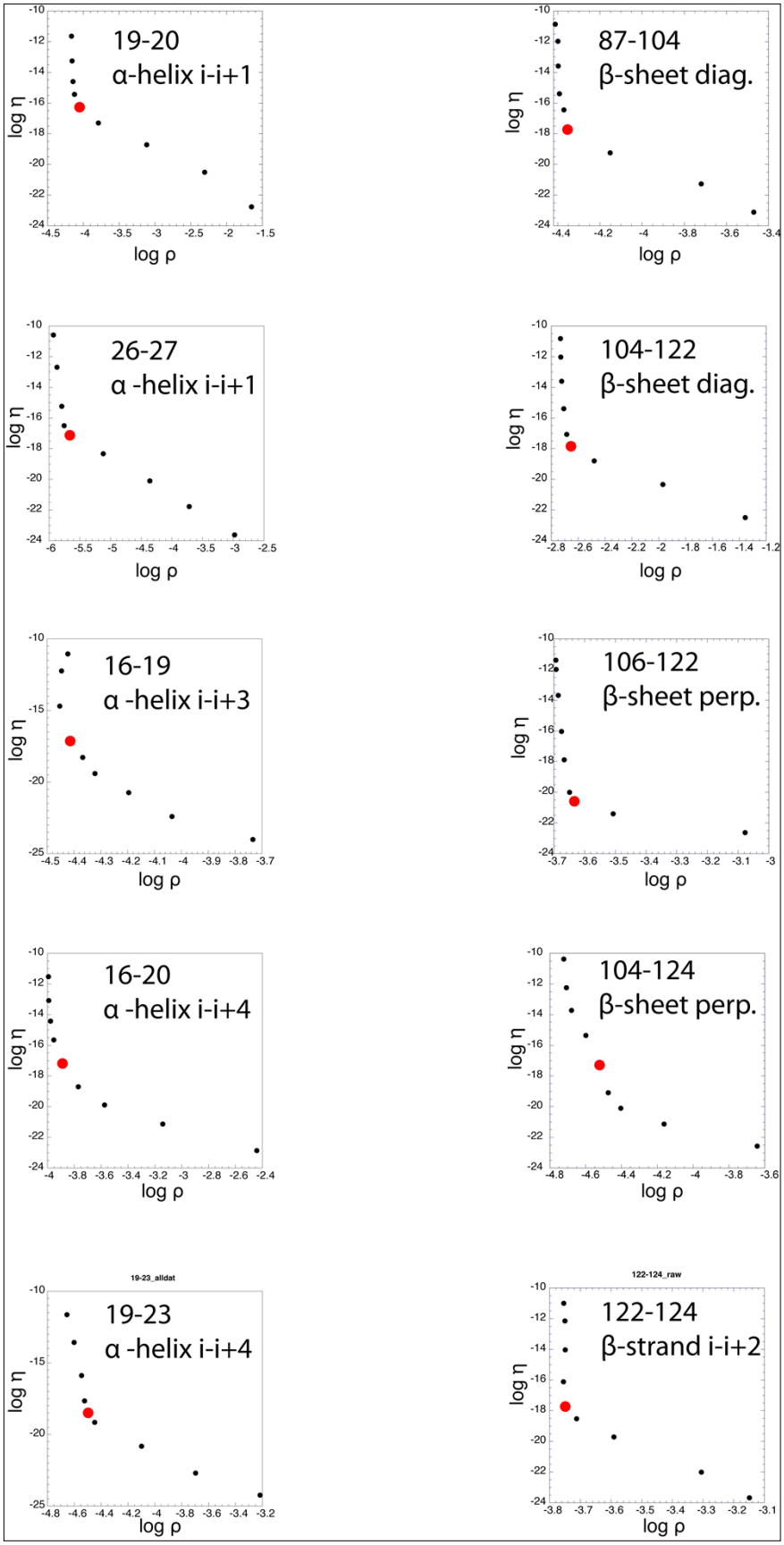

Fig. S6. L-curves comparing the smoothness of the distance distribution to the mean square deviation for the 10 Rx labeled positions. The chosen alpha terms are indicated by red points on each curves.

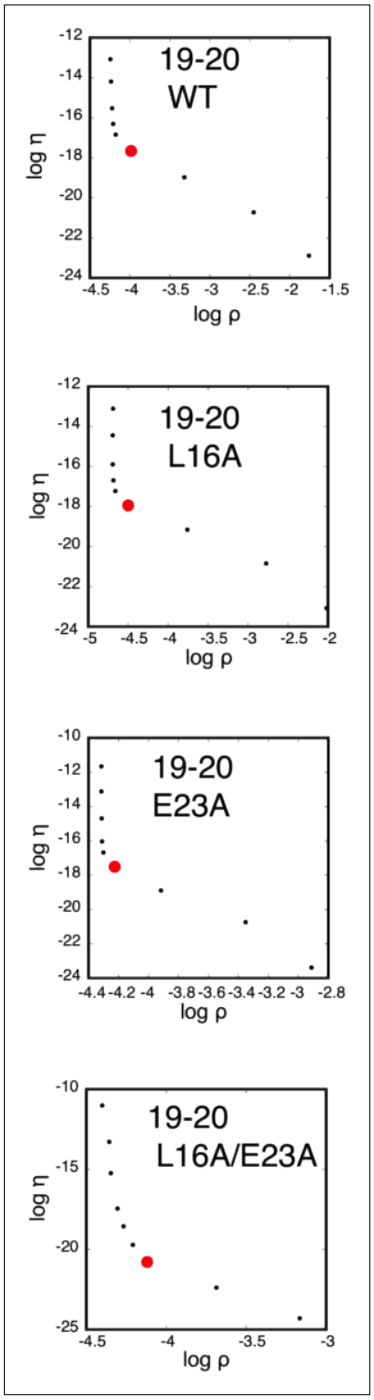

Fig. S7. L-curves comparing the smoothness of the distance distribution to the mean square deviation for Rx position 19-20 and constructs with mutated flanking residues. The chosen alpha term is indicated by a red point on each curve.

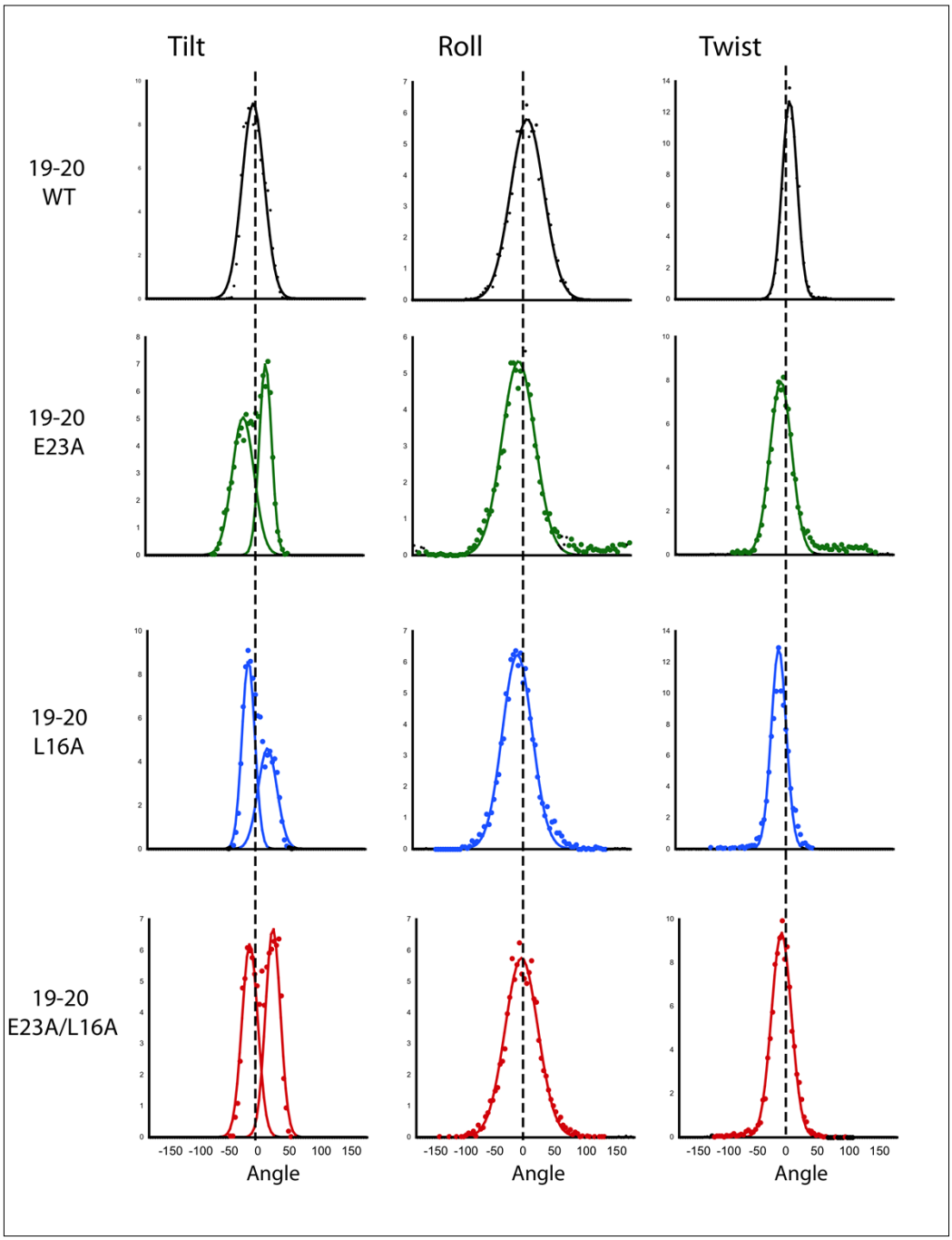

Fig. S8. Extracted angle distributions for the spin labels of the mutations around 19-20, in the order Tilt, Roll and Twist. Binned values are shown as dots and fitted Gaussian curves are shown as continuous lines. The color scheme corresponds to that used in figure 4.

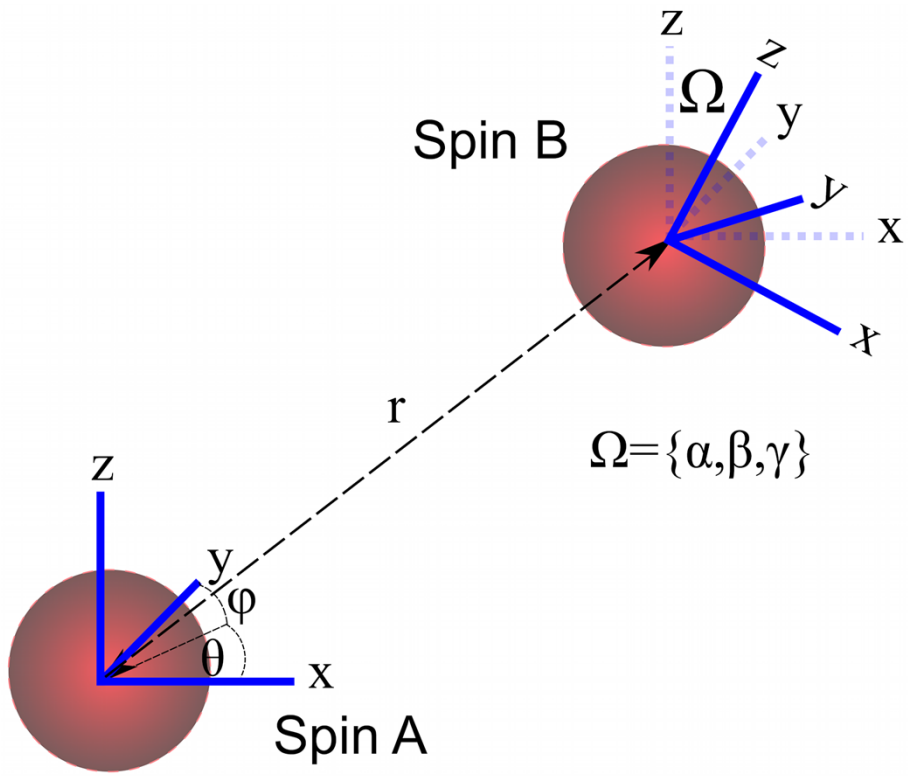

Fig. S9 The angular relationship between the spin-pairs

S2 Comparison of experimental data, fitted results, PELDOR simulations of MD and random orientation.

A comparison between the results from analyzing the experimental data, simulation of the PELDOR signal, corresponding to the MD frames and that of a random orientation distribution (the case where there is no spin-spin orientation correlation) was made at stages in the analysis.

The PELDOR modulation depth analysis was performed so as to calculate the RMSD between experimental modulation depths and a simulated library and to use the lowest RMSD values as initial values for a fitting algorithm.

By simulation of the modulation depth for each experiment, over a uniformly spaced set of Euler angles, we can produce a measure of RMSD of modulation depths between the simulated orientations from the uniform angle set and the experimental values. In this way we can use the RMSD to produce a two dimensional plot, which indicates the orientations having the smallest RMSD (orientations where the simulated modulation depths are closest to the experimental ones). In the fig. S10 we show which of the relative N-O vector directions between spin labels have the smallest RMSD. The grey-scale plot in the background shows the RMSD values normalized to maximum value derived from the RMSD between a large-scale library of modulation depths and the experimental measured modulation depths. The grey scale was chosen such that white corresponds to the minimum RMSD value found and black corresponds to the largest RMSD value. The 5 uniform spaced red contours indicated the density of relative N-O bond angles calculated from the MD simulation. Due to the numerous symmetries there are several peaks shown in the RMSD plots, and these have been extracted and presented in supplementary material Table S2 as 16 ZYZ Euler angles.

These angles are then used as initial values for the fitting method described earlier to produce refined relative orientation angles and distributions; these are shown in table 2. Spherical density plot of relative spin-spin N-O vector directions for the fitted distribution is shown in fig 7 along with the equivalent distribution obtained from the MD frames. For both mutants there is a reasonable overlap between the Contours derived from the MD frames and the contours derived fro the RMSD fitting.

A simulation of the: PELDOR signals corresponding to the MD simulation, a random distribution of rotation angles between each spin and the PELDOR signal for the analysis derived model of the spin label pair were compared to experimental PELDOR signals, shown in fig. 6

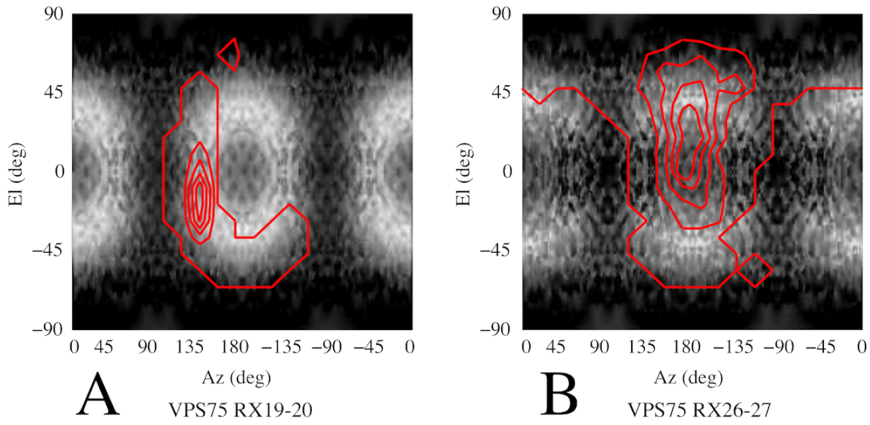

Fig. S10 Two-dimensional greyscale plots showing the RMSD values between a library of simulated relative spin label orientations and the experiment measured modulation depth values. The scale is normalized such that white corresponds to the smallest RMSD value and black corresponds to the largest. Overlaid is a red contour plot of the density of relative orientations derived from the MD simulations. (A) Rx19-20 result (B) Rx26-27.

Alpha (Z)	Beta (Y)	Gamma (Z)
135.0	41.0	-135.0
48.8	130.0	-138.8
-41.2	50.0	-131.2
-135.0	139.0	-135.0
135.0	139.0	-45.0
48.8	50.0	-41.2
-45.0	139.0	-45.0
-135.2	41.3	-45.3
135.2	41.3	45.3
45.3	139.2	45.3
-45.3	41.3	45.3
-135.2	139.2	45.3
135.2	139.2	135.2
45.3	41.3	135.2
-45.3	139.2	135.2
-135.2	41.3	135.2

Alpha (Z)	Beta (Y)	Gamma (Z)
-146.3	129.0	-146.3
33.7	129.0	-146.3
-33.7	51.0	-146.3
146.3	51.0	-146.3
-146.3	51.0	-33.7
-33.7	129.0	-33.7
33.7	51.0	-33.7
146.3	129.0	-33.7
-146.3	129.0	33.7
-33.7	51.0	33.7
33.7	129.0	33.7
146.3	51.0	33.7
-146.3	51.0	146.3
-33.7	129.0	146.3
33.7	51.0	146.3
146.3	129.0	146.3

Table S2. All the angles corresponding to the RMSD minimum found in the analysis of the RMSD values between a library of simulated relative spin label orientations and the experiment measured modulation depth values. 16 Solutions are found which is consistant with experiment symmetry.

gxx	2.0091
gyy	2.0072
gzz	2.00341
Axx (Mhz)	14.7
Ayy (MHz)	16
Azz (MHz)	97.8
Main coil field (Gauss)	33435

Table S3 The values of the g-tensors and hyperfine coupling (MHz) for sample RX19-20 were found by fitting to pulsed W-band field-swept echo spectra obtained

using selective pulses with the Pi pulse length being 100ns to reduce excitation and thus instantaneous diffusion effects. The fitting was performed using the high performance EasySpin package [7].

gxx	2.0091
gyy	2.0072
gzz	2.00341
Axx (Mhz)	14.7
Ayy (MHz)	16
Azz (MHz)	97.8
Main coil field (Gauss)	33425

Table S4 The values of the g-tensors and hyperfine coupling (MHz) for sample RX26-27 were found by fitting to pulsed W-band field-swept echo spectra obtained using selective pulses with the Pi pulse length being 100ns to reduce excitation and thus instantaneous diffusion effects. The fitting was performed using the high performance EasySpin package [7].

Probe pulse 1 length (ns)	**Probe pulse 2 length (ns)**	**Pump pulse 1 length (ns)**	**Probe pulse 3 length (ns)**	**Offset coil (Gauss)**	**Probe frequency (GHz)**	**Pump frequency (GHz)**
10	20	17	20	0	93.9996	93.93
10	20	15	20	0	93.9996	93.87396
10	20	15	20	0	93.9996	93.78996
10	20	18	20	0	93.9996	93.70596
10	20	21	20	35	93.9996	94.098
10	20	20	20	35	93.9996	94.07004
10	20	15	20	35	93.9996	93.90204
10	20	15	20	35	93.9996	93.804
10	20	25	20	80	93.9996	94.224
10	20	22	20	80	93.9996	94.14
10	20	23	20	80	93.9996	94.11204
10	20	20	20	80	93.9996	94.07004
10	20	15	20	80	93.9996	93.93

Table S5 Table of experiment parameters, pulse lengths, magnetic field offsets and pulse excitation frequencies for w-band experiments on attachment site 19-20 site.

Probe pulse 1 length (ns)	Probe pulse 2 length (ns)	Pump pulse 1 length (ns)	Probe pulse 3 length (ns)	Offset coil (Gauss)	Probe frequency (GHz)	Pump frequency (GHz)
5.5	11	11	11	78	93.9996	94.12596
5.5	11	11	11	78	93.9996	94.19604
5.5	11	11	11	130	93.9996	94.11204
12	24	24	24	22	93.9996	93.93
5.5	11	11	11	105	93.9996	94.11204
12	24	24	24	-5	93.9996	93.93
5.5	11	11	11	0	93.9996	93.90204

Table S6 Table of experiment parameters, pulse lengths, magnetic field offsets and pulse excitation frequencies for w-band experiments on attachment site 26-27 site.

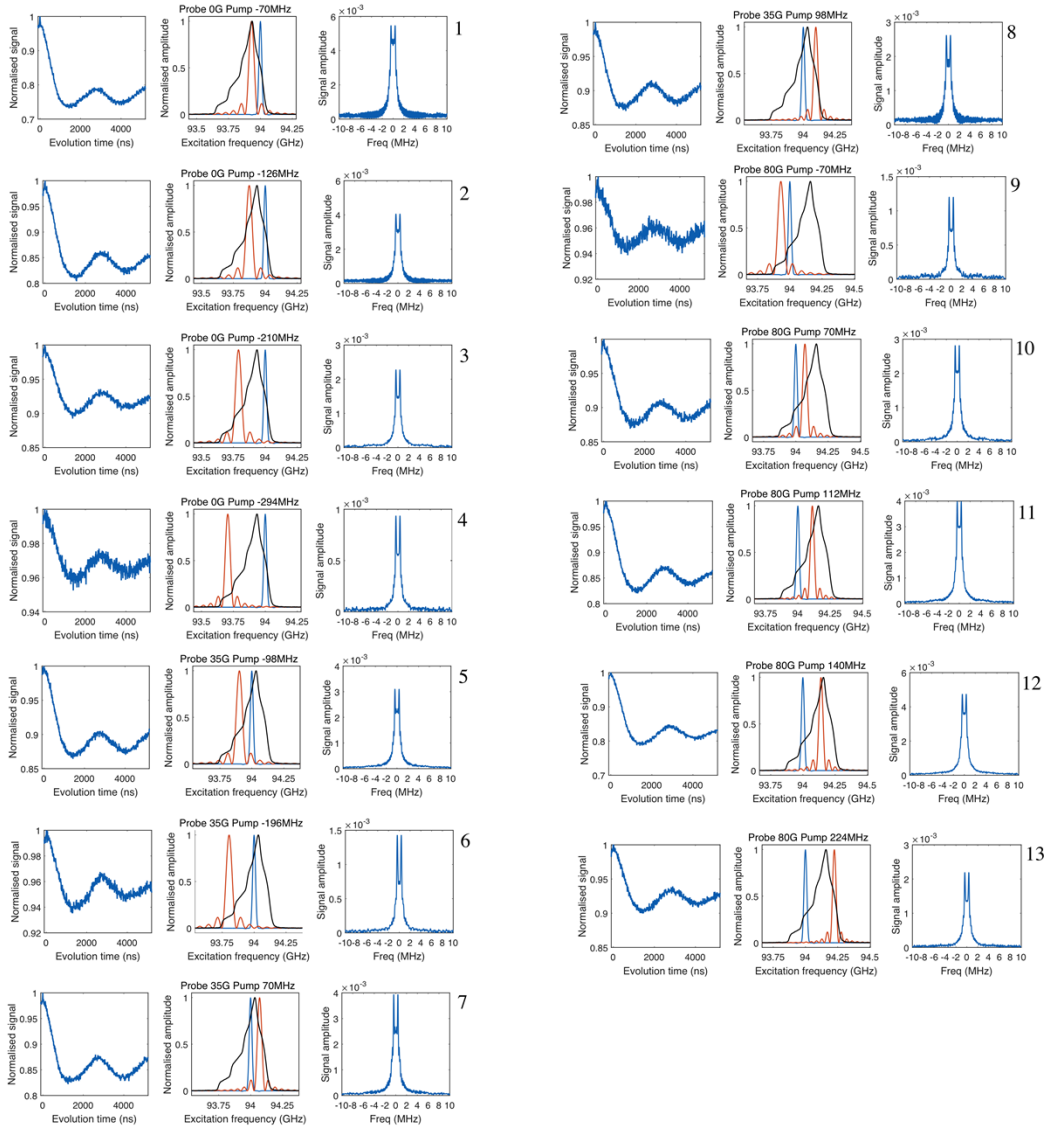

Fig S11 Experimental PELDOR signal (left), pulse excitation overlaid on the RX spin label spectrum (middle) and FFT of the PELDOR signal (right) are shown for each w-band orientation selective PELDOR experiment of sample RX19-20. In the pulse

excitation diagrams the blue line represents the probe pulse (in Gauss) and the red line represents the pump pulse represented as an offset (in MHz) from the probe position. Diagram order corresponds to the order in fig. 6

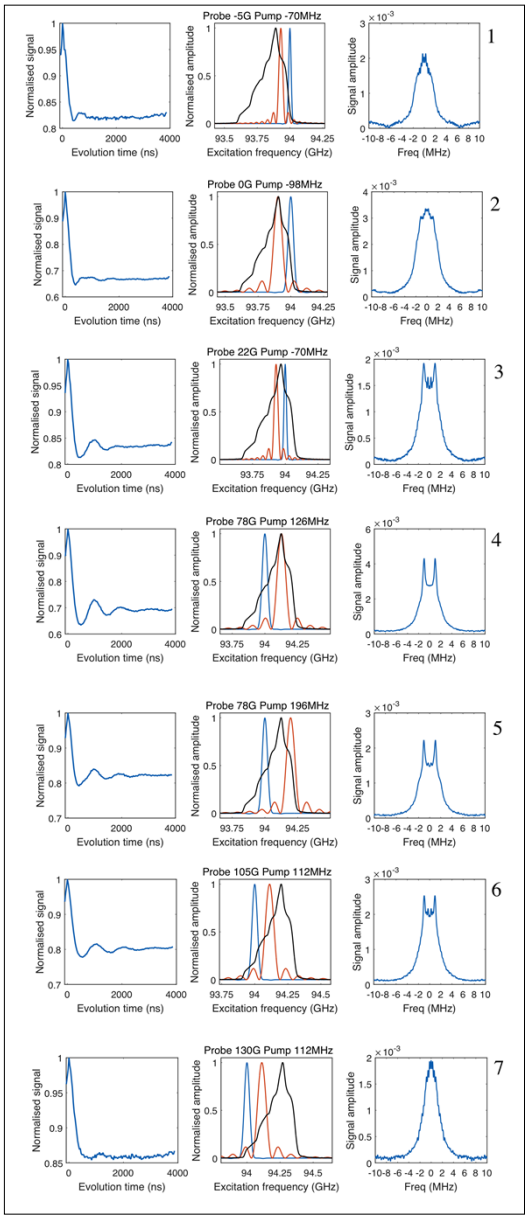

Fig S12 Experimental PELDOR signal (left), pulse excitation overlaid on the RX spin label spectrum (middle) and FFT of the PELDOR signal (right) are shown for each w-band orientation selective PELDOR experiment of sample RX26-27. In the pulse excitation diagrams the blue line represents the probe pulse (in Gauss) and the red line represents the pump pulse represented as an offset (in MHz) from the probe position. Diagram order corresponds to the order in fig. 6

References

1. E. Gasteiger, A. Gattiker, C. Hoogland, I. Ivanyi, R. D. Appel and A. Bairoch, *Nucleic Acids Research*, 2003, **31**, 3784-3788.
2. P. A. S. Cruickshank, D. R. Bolton, D. A. Robertson, R. I. Hunter, R. J. Wylde and G. M. Smith, *Rev Sci Instrum*, 2009, **80**.
3. M. Bak and N. C. Nielsen, *J Magn Reson*, 1997, **125**, 132-139.
4. V. B. Cheng, H. H. Suzukawa and Wolfsber.M, *J Chem Phys*, 1973, **59**, 3992-3999.
5. P. C. Kahn, *Comput Chem*, 1989, **13**, 185-189.
6. G. Jeschke, V. Chechik, P. Ionita, A. Godt, H. Zimmermann, J. Banham, C. R. Timmel, D. Hilger and H. Jung, *Appl Magn Reson*, 2006, **30**, 473-498.
7. S. Stoll and A. Schweiger, *J Magn Reson*, 2006, **178**, 42-55.